Review History for “Shear strength of angular granular materials with size and shape polydispersity”

Sergio Andres Carrasco Cisterna, David Cantor, Carlos Ovalle, Paula Quiroz-Rojo

2023

Summary (optional)

The paper was sent to three reviewers — Dr. Vasileios Angelidakis (Reviewer A), Dr. Debdeep Sarkar (Reviewer B) and Dr. Francois Guillard (Reviewer C). The reviewers remained anonymous during the entire review process and the authors were anonymous for the reviewers. After the reviewing process was complete, both reviewers agreed to disclose their identity. In Review Round 1, the reviewers provided a series of comments for the authors and required a revision of the manuscript. In Review Round 2, the reviewers recommended the manuscript for publication.

Review Round 1

Reviewer 1 (Vasileios Angelidakis)

I have reviewed this manuscript exploring the critical-state shear-strength characteristics of polydisperse packings with polygons of variable shape sharpness and irregularity. The authors have conducted a well-designed parametric study via two-dimensional Contact Dynamics simulations, where two aspects of particle shape are varied systematically, for a wide range of particle size polydispersity. I found the analysis informative and the manuscript is written very clearly. I raise a few points for the consideration of the authors.

Technical comments:

- Abstract + L518: In several parts of the manuscript it is claimed that irregularity has a less pronounced effect than the sharpness of corners. I agree this is evidenced by the results of the current study, but I am not sure if this is a generalisable result. For instance, (I think) your parameterisation of irregularity does not allow for particles of very high aspect ratio. This makes me think, have these two aspects of particle shape been varied by comparable ranges or is this a limitation of the way you parameterize sharpness and irregularity? I am curious to get the opinion of the authors on this.

- L305: I would rephrase to "average number of contacts per load-bearing grain" or similar, to clarify this is not the average coordination number (that would include the rattlers). Your definition of Z seems to be similar to the mechanical coordination number, as in Thornton [1], if Nc does not include the contacts of grains with just one contact. Are they the same descriptor or do Nc include all contacts with non-zero force?

- Figure 12(b) and (c): Since the results for the two cases look similar, and almost linear, would it be of interest to try and find a linear relationship of (S,dr) that describes/collapses all the curves? Could such a relationship serve as a predictive tool for your system?

- In the manuscript, the parameters for shape irregularity, shape sharpness and size polydispersity are employed with good effect. However, these are tailored for this specific type of particles. Would the authors be interested to replot 1-2 of their most interesting graphs using parameters typically used to characterise irregular particles? E.g., Wadell's circularity [2], Wadell/Wenworth's [3] roundness or D50 + uniformity coefficient Cu=D60/D10?

Minor edits:

- L279: typo "a similar trends" - L340: I would say "an almost linear". - Figure 12(a): Seems like there is a typo in the legend of the lines, should say Case 2A and Case 2B - L491: Please replace "y" with its English counterpart

[1] C. Thornton, Geotech. 50 (1) (2000) 43-53. [2] H. Wadell, J. Geol. 40 (5) (1932) 443–451. [3] C.K. Wentworth, J. Geol. 27 (7) (1919) 507–521.

Reviewer 2 (Debdeep Sarkar)

The paper deals with using DEM to simulate different grain shapes and sizes on the static behavior of soils. In general, the paper is well presented, clearly written and delivers solid information. I have some comments and clarifications though for the paper for improvement.

In literature section, the authors have stated possible reasons for discrepancies in experimental observations in shear strengths. This could also result on what basis are the shear strengths compared, if they are compared at similar void ratio or relative density. Different grain sizes will have slightly different limit void ratios, although the values are more dependent on the uniformity coefficient (Youd 1973, Zheng and Hryciw, 2016, Sarkar et al 2019). Furthermore, typically smaller samples show larger shear strength than larger samples owing to boundary conditions. These points may also be mentioned to provide the readers as to why such contradictions exist. Also grain crushing is a phenomenon typically observed in carbonate sands at lower stresses or quartz sands at higher stresses over 10 MPa.

The authors must comment on why 2D grains are used instead of 3D given the significant improvement in capturing real grains via spherical harmonics or micro CT scan photos. The grain shapes used are not exactly represetative of what is encountered in nature.

In sample preparation by depositional algorithm, it is not clear if air pluviation or dry depostion techniques are meant. It must be clarified. What was the specific density of grains used (usually 2650 kg/m3)?

How do you define critical state in the DEM simulation- is it when you reach a specific axial strain or you reach constant values of q/p or a constant CN? Also does all the tested materials in simulation achieve critical state at similar axial strains?

The coordination number Z = 2Nc/Np is it the mechanical coordination number? Because as far as I remember, mechanical CN has a slightly different formulation that stated here.

I would also like to see a couple of q/p profile against the axial strain for some cases as they impart a lot of information on strain hardening/softening tendency. Or the variation of the CN against axial strain.

Reviewer 3 (Francois Guillard)

This paper simulates two-dimensional angular grains using contact dynamics in a simple shear configuration. The interplay between grain-size distribution and angularity is studied by shearing samples ranging from monodisperse to widespread size distribution, where the prescribed angularity of the grains is related to their size. In addition, the role of the irregularity of the polygons making the grains is explored. Volume fraction, coordination number, and frictional properties are reported for each sample, as well as the stress partition between species. The results show significant effects of the size distribution, angularity, and irregularity of the grains on the material's mechanical response. These interesting results represent a step towards a better understanding of those complex interplays. While the applicability of the results to geomechanical problems is still remote, especially given that the simulations are two-dimensional, the paper can be of broad enough interest to warrant publication in Open Geomechanics, if the comments below are addressed.

1/ It would be good to clarify what is exactly the system when S=0. For case A 1A for example, is it a mixture of the 10 shapes, all with the same "diameter"? Then the total area of each shape would need to be the same, leading to more triangles than 64-sides polygons. Is that correct?

2/ Tying up to the previous question, I find the drop in Fig. 9b between S=0 and S=0.1 quite surprising, and inconsistent with the rest of the trend. Any idea why the volume fraction is changing so much when adding a little polydispersity for the irregular pentagons, while it was pretty stable for the cases with different shapes?

3/ It is a missed oportunity in my mind not to show the beginning of the simulations before reaching critical state in figure 7. It is nice to see that the steady state is reached and stable, but there would be room to show how we got there.

4/ Part of the discussion on how Zf depends on the size and sharpness should consider that for the same dr, the length of the side of the particle depends on the number of sides of the polygon. Triangles have intrinsically less surface to establish contact than disks for a given circumscribing diameter. Therefore it may be good to also show the distributions of Zf as a function of perimeter length, to distinguish between the size effect and the sharpness effect on Zf. Also, the case S=0 is absent from the graphs in Fig 11, but there could still be differences in Zf between the different shapes of equal diameter grains (if my interpretation in (1) is correct), and it would be good to report it too.

5/ Considering the vertex-side and side-side split of the stresses (Fig. 15), these reproduce the behaviour of the number of contacts. Is there any difference in the typical intensity of the forces that each type of contact carries?

6/ I need clarification on how the stress partition by shape is performed. How are the q_i computed? Does this include any contact with one of the particles of the given shape? Also, it would be interesting to report the normal stress partition as well as the deviatoric stress, since a priori there is no reason to have equipartition of the stresses between species. Actually, regarding normal stress and pressure, would it be possible to also show (maybe in figure 7) how well the prescribed pressure is maintained and how close p and P are to each other?

7/ The mathematical definition of the "regularity" of the pentagons given in eq. (1) is not specified enough. Is the plus-minus sign based on the value of k? For delta=1, which is used in some simulations, the equation would generate a triangle, which is not what Fig. 2 shows.

8/ Eq. 3 and Eq. 6 basically define two different notation for the same quantity. It would be clearer to introduce first the relative diameter d_r, and then rewrite equations 3 and 4 in terms of this d_r as either $\delta=d_r$ or $\delta=1-d_r$.

Miscellaneous:
Fig 3 caption: The writing is a bit unclear, suggesting that S is normalised by d_max (while it is d that is normalised).
l. 192: "As/A" -> "A_s/A"
l. 204: which kind of average is considered here for <d>, the area average?
Fig 6 caption: "x' axis" -> "x axis"
l. 217: "as they were glued" -> "as if they were glued"
Fig 11a inset y-label: "C_0" -> "c_0"
l. 550: "q_sc" -> "q_i"

Author Response

We thank both reviewers. When Reviewer 1 says:

Please change XYZ

We fixed it.

Responses to the Reviewer A:

We thank the Referee for the attentive reading of our manuscript and the useful comments. Please find each of the comments (#) followed below by our answers (A#).

1. Abstract + L518: In several parts of the manuscript it is claimed that irregularity has a less pronounced effect than the sharpness of corners. I agree this is evidenced by the results of the current study, but I am not sure if this is a generalisable

result. For instance, (I think) your parameterisation of irregularity does not allow for particles of very high aspect ratio. This makes me think, have these two aspects of particle shape been varied by comparable ranges or is this a limitation of the way you parameterize sharpness and irregularity? I am curious to get the opinion of the authors on this.

A1. The referee is correct in pointing out that the shape parametrization in this work does not allow particles to exhibit large aspect ratios. However, the effect of particle aspect ratio on shear strength was already addressed by Carrasco et al. (2022) [1], discovering that when the particle size and aspect ratio are correlated, the shape of the smallest particles consistently has a significant impact on the shear strength of the granular material. Since particle aspect ratio and angularity are two shape properties that can affect the shear strength properties differently, it is key to explore each geometrical aspect separately to fully understand the mechanical behavior of these materials.

2. L305: I would rephrase to "average number of contacts per load-bearing grain" or similar, to clarify this is not the average coordination number (that would include the rattlers). Your definition of Z seems to be similar to the mechanical coordination number, as in Thornton [1], if Nc does not include the contacts of grains with just one contact. Are they the same descriptor or do Nc include all contacts with non-zero force?

A2. We thank the Referee for this remark. For the sake of clarity, we modified line 348 in the paper as suggested:

L348: [...] or average number of contacts per load-bearing grain.

Regarding the Referee's question about the similarity of our coordination number and that of Thornton [2], let us point out some key differences. In Thornton's work, the mechanical coordination is defined as:

$$Z_m = \frac{2C - N_1}{N - N_1 - N_0}, \tag{1}$$

being C the number of contacts, N the number of particles, and N_1 and N_0 the number of particles with only one or no contacts, respectively. On the other hand, the coordination number in this work is defined as:

$$Z = \frac{2Nc}{N_p^*} \tag{2}$$

where N_c is the total number of force-bearing contacts (i.e., all contact with non-zero force), and N_p^* is the number of grains transmitting forces (i.e., particles with two or more non-zero force contacts). There is, hence, a slight difference between the two definitions, primarily related to the treatment of N_1 in Eq. (1). To illustrate this, Figure 1 shows the evolution of Z and Z_m for Case 1A and Case 1B in our simulations, where we can observe that Z_m is consistently slightly higher than Z. This difference arises from the fact that we do not consider gravity in our simulations. In simulations where gravity is activated, such as in Thornton's work, both parameters should yield the same values. Nevertheless, despite this discrepancy, Z_m and Z show similar values and display comparable trends with S, allowing us to draw similar conclusions regardless of which one we choose to use.

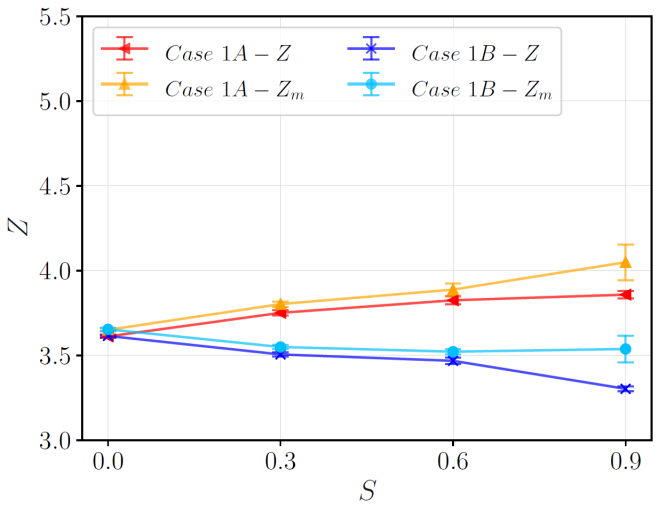

Figure 1: Evolution of Z and Z_m for Case 1A and 1B as a function of particle size span S.

3. Figure 12(b) and (c): Since the results for the two cases look similar, and almost linear, would it be of interest to try and find a linear relationship of (S,dr) that describes/collapses all the curves? Could such a relationship serve as a predictive tool for your system?

A3. We thank Referee for this interesting request. Although the similarities in Figs. 12 (b) and (c) may suggest this behavior could be summarized through a predictive relationship, we were not able to identify a reliable set of hypotheses to develop such a predictive tool. For instance, it is not possible to infer the coordination number values in the extreme cases (i.e., when $dr = 0$ or $dr = 1$) when particle size and shape are continuously changing. Additionally, we could not find any analytical base or normalization to predict the different slopes of the curves. Further analyses would be necessary to gain a deeper understanding of the microstructural origins underlying this simple linear evolution of Z_f with dr while considering varying grain size span S.

4. In the manuscript, the parameters for shape irregularity, shape sharpness and size polydispersity are employed with good effect. However, these are tailored for this specific type of particles. Would the authors be interested to replot 1–2 of their most interesting graphs using parameters typically used to characterise irregular particles? E.g., Wadell's circularity [2], Wadell/Wenworth's [3] roundness or D50 + uniformity coefficient Cu=D60/D10?

A4. As suggested by the Referee, we compared the grain size span parameter S with the D_{50}, the uniformity coefficient ($C_u = D_{60}/D_{10}$), and the ratio between the maximum to minimum particle sizes ($RD = D_{100}/D_0$). These parameters are presented in Table 1 below, which is also included in the manuscript on line 192. It is important to note that these parameters are all related to the grain size distribution and do not consider the particle shape.

Table 1: Parameters $d_{\max}$, $d_{\min}$, R_D, D_{50} and C_u for different values of S.

S	$d_{\max}\,[mm]$	$d_{\min}\,[mm]$	R_D	$D_{50}\,[mm]$	C_u
0	15.0	15.0	1.0	15.0	1.0
0.1	15.0	12.3	1.2	13.7	1.1
0.2	15.0	10.0	1.5	12.5	1.2
0.3	15.0	8.1	1.9	11.5	1.4
0.4	15.0	6.4	2.3	10.7	1.6
0.5	15.0	5.0	3.0	10.0	1.8
0.6	15.0	3.8	4.0	9.4	2.2
0.7	15.0	2.7	5.7	8.8	2.6
0.8	15.0	1.7	9.0	8.3	3.2
0.9	15.0	0.8	19.0	7.9	4.2

We also decided to replot Figures 9 (shear strength) and 10 (solid fraction) of the manuscript as a function of C_u (Figure 2 below). As the relationship between S and C_u is not linear, a slight difference can be observed under this new visualization. Nevertheless, the observations and conclusions drawn from these plots stay the same. Considering the Wadell-Wenworth's roundness parameter, as suggested by the Referee, let us recall its definition as

$$P = \frac{1}{N}\sum\frac{r_i}{R}, \tag{3}$$

where r_i is the radius of curvature of any particular edge on the grain, R is the radius of the inscribed circle within the grain, and N is the number of edges measured. Unfortunately, this parameter is not applicable to the current study since the corners of the grains are perfectly sharp, so $r_i = 0$ for all the shapes considered.

On the other hand, Wadell's circularity ϕ_w is an interesting parameter that allows for the comparison of particle shapes in all the cases considered in this study. The definition of this parameter being as follows:

$$\phi_w = \frac{c}{C}, \tag{4}$$

where c is the perimeter of a circle of the same area as the plane figure, and C is the actual perimeter of the plane figure [3]. In Case 1, ϕ_w evolves from 0.77 for triangular particles to 0.99 for polygon with 64 sides. In Case 2, ϕ_w varies from 0.93 for regular pentagons to 0̃.905 for the most irregular pentagonal shape. These observations are now mentioned in the line 181 of the manuscript:

L181: [...] In terms of Wadell's circularity, defined as $\phi_w = c/C$, being c the perimeter of a circle of the same area as the plane figure, and C is the actual perimeter of the plane figure [3], Case 1 shows ϕ_w evolving from 0.77 for triangles to 0.99 for

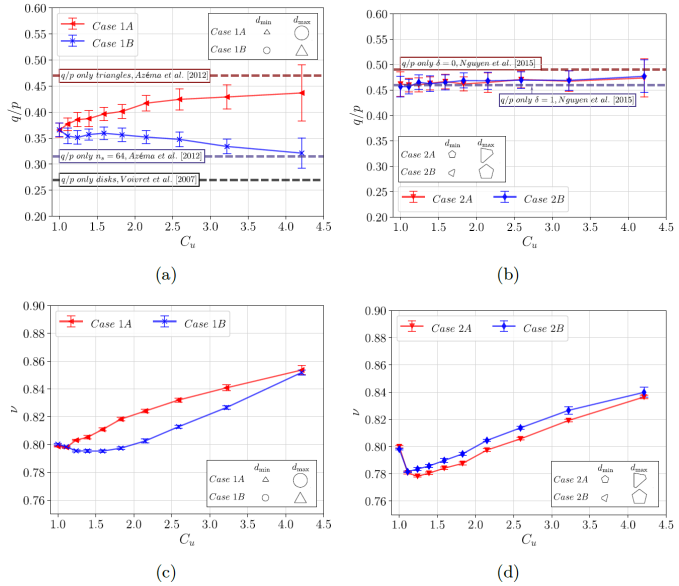

Figure 2: Evolution of the average of q/p and ν as a function of the particle size dispersion S for Case 1 (left) and Case 2 (right). Error bars display the standard deviation of the data.

polygons with 64 sides. In Case 2, ϕ_w varies from 0.93 for regular pentagons to $\tilde{0}$.905 for the most irregular pentagon.

We also decided to replot Figures 11 and 12 in the manuscript as a function of ϕ_w (Figure 3 below). For Case 1, these plots show the counterintuitive observation that larger particles with high values of ϕ_w (i.e., more circular) are consistently better connected than larger sharper particles. For the class of smaller particles, the less circular grains tend to be more connected. Nevertheless, the grain size is the parameter mainly driving the larger variations in particle connectivity. Considering the relevance of Wadell's circularity parameter to this topic, we decided to include Figures 3 as insets in Figures 11 and 12 in the manuscript.

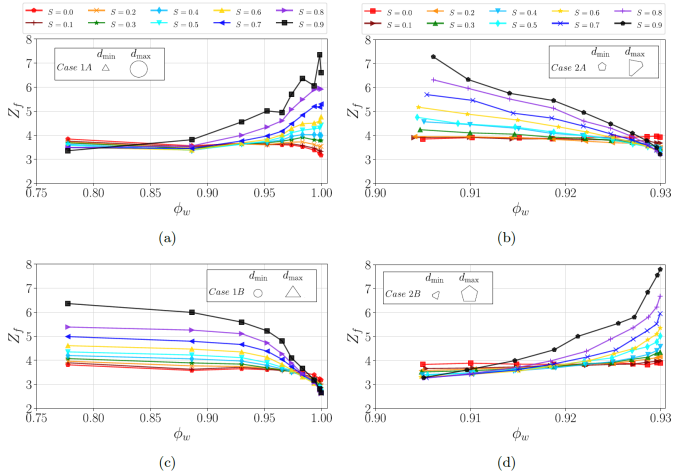

Figure 3: Evolution of the coordination by family of particle Z_f at critical state as a function of the Wadell's circularity ϕ_w and for Case 1A (a), Case 1B (c), Case 2A (b) and Case 2B (d).

We also modified line 385 of the manuscript as follows:

L385: If we compare Z_f in inset figures of Cases 1A and 1B, larger particles with high n_s are always better connected than larger sharper particles, as opposed to the smaller particles where less circular grains tend to be more connected. This behavior is presumably due to the capacity of small sharper particles to reach neighboring particles with their corners that are

normally unreachable for less angular grains [4].

Minor edits:

We thank the referee for the set of minor comments. The corresponding modifications were made in the manuscript for the following lines.

- L279: typo “a similar trends”
- L340: I would say "an almost linear".
- Figure 12(a): Seems like there is a typo in the legend of the lines, should say Case 2A and Case 2B
- L491: Please replace "y" with its English counterpart

Responses to the Reviewer B:

We thank the Referee for the attentive reading of our manuscript and the useful comments. Please find each of the comments (#) followed below by our answers (A#).

1. In literature section, the authors have stated possible reasons for discrepancies in experimental observations in shear strengths. This could also result on what basis are the shear strengths compared, if they are compared at similar void ratio or relative density. Different grain sizes will have slightly different limit void ratios, although the values are more dependent on the uniformity coefficient (Youd 1973, Zheng and Hryciw, 2016, Sarkar et al 2019). Furthermore, typically smaller samples show larger shear strength than larger samples owing to boundary conditions. These points may also be mentioned to provide the readers as to why such contradictions exist. Also grain crushing is a phenomenon typically observed in carbonate sands at lower stresses or quartz sands at higher stresses over 10 MPa.

A1. We thank the Referee for these remarks. We decided to split this comment into three main points, each one of them leading to clarifications or further explanations in the manuscript as follows.

1. “This could also result on what basis are the shear strengths compared, if they are compared at similar void ratio or relative density. Different grain sizes will have slightly different limit void ratios, although the values are more dependent on the uniformity coefficient (Youd 1973, Zheng and Hryciw, 2016, Sarkar et al 2019)”

   L36: [...] Moreover, using the relative density as a basis for shear strength comparison is not the most appropriate because different particle size distribution (psd) have different density limits [5, 6].

2. “typically smaller samples show larger shear strength than larger samples owing to boundary conditions.”

   L44 [...] Finally, the aspect ratio between the maximum particle size and the characteristic sample size, which is known to have a significant impact on the strength [7, 8, 9].

3. “Also grain crushing is a phenomenon typically observed in carbonate sands at lower stresses or quartz sands at higher stresses over 10 MPa.”

   L40 [...] In addition, materials can undergo grain crushing at certain stress levels depending on their particle strength, which implies lower dilatancy and, thus, a reduced peak strength [10, 11, 12].

2. The authors must comment on why 2D grains are used instead of 3D given the significant improvement in capturing real grains via spherical harmonics or micro CT scan photos. The grain shapes used are not exactly represetative of what is encountered in nature.

A2. We thank the Referee for this comment. Due to the lack of research and works focused on the effects of size-shape correlations (both experimental and numerical), we decided to start this campaign of numerical tests using the simplest model possible. Our aim was to clearly describe grain shape and size variations while using the minimum number of parameters. In addition, we purposely used 2D geometric shapes with line segments as sides and a constant coefficient of friction. This choice allowed us to carefully control the interactions between grains and completely isolate the effect of the size-shape correlations. To further validateour 2D simulations and enable direct comparisons with physical experiments or materials in the field, which the Referee has highlighted, we are currently invested in developing such three-dimensional simulations and look forward to gaining new insights into the mechanics of realistic granular materials.

3. In sample preparation by depositional algorithm, it is not clear if air pluviation or dry depostion techniques are meant. It must be clarified. What was the specific density of grains used (usually 2650 kg/m3)?

A3. The construction of the samples is based on a sequential protocol that consists of a layer-by-layer deposition of rigid particles on a substrate, based on geometrical rules [13, 14, 15]. The protocol is based on a potential energy deposition strategy, where each particle is placed in the lowest position on the free surface as a function of its diameter. This approach aims to minimize the potential energy $\Psi = \sum_{i=1}^{N_p} y(i)$, being $y(i)$ the vertical coordinate of particle i (see Fig. 4 (a)). This approach allows the free surface of the packing to remain nearly flat and horizontal compared to other protocols [14, 13]. Although particle deposition can also be simulated using dynamic methods in order to replicate air pluviation or dry deposition, such simulations typically require larger computation times compared to the purely geometrical approach used in this work. Finally, it important to note that this research focuses on the characterization of the mechanical response in the critical state, which is independent of the initial packing density of the specimens.
The specific density of grains used was 2000 kg/m^3.

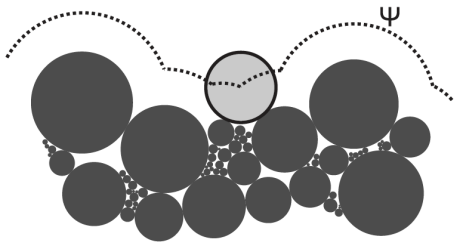

Figure 4: (a) Illustration of potential-based deposition method [13].

To clarify this construction step of the samples, we modified the line 216 in the paper as follows:

L216: Each numerical sample is built with $N_p \approx 10\,000$ particles, which are placed layer-by-layer in boxes by mean of a potential energy deposition protocol as described in Ref. [13, 14, 15]. This approach is an efficient strategy to achieve relatively dense random packing configurations without the need of time consuming dynamic simulations.

4. How do you define critical state in the DEM simulation- is it when you reach a specific axial strain or you reach constant values of q/p or a constant CN? Also does all the tested materials in simulation achieve critical state at similar axial strains?

A4. In this work, the critical state is considered as the state where plastic shear deformations occur indefinitely without changes neither in volume nor stress state [16, 17]. In other words, we consider that the samples are in the critical state when they reach constant values of q/p and solid fraction ν under continuous shear deformation γ. We also verify that the coordination number reaches a steady value around the same levels of deformation as the macroscopic parameters.

Figure 5 shows the evolution of the shear strength q/p for all cases as functions of the shear deformation γ. We observe that q/p generally increases up to γ 0̃.2. Then, a transient regime towards the steady state is observed, with its extent depending on the material. In Case 1A, the steady state is reached at approximately γ 0̃.4, while in Case 1B, the stabilization appears more rapidly, around γ 0̃.3. For Cases 2A and 2B, the stabilization of shear strength occurs practically at same deformation levels (around γ 0̃.3). Regarding the volume of the sample, it is noteworthy that the solid fraction reaches steady values systematically earlier than the shear strength.

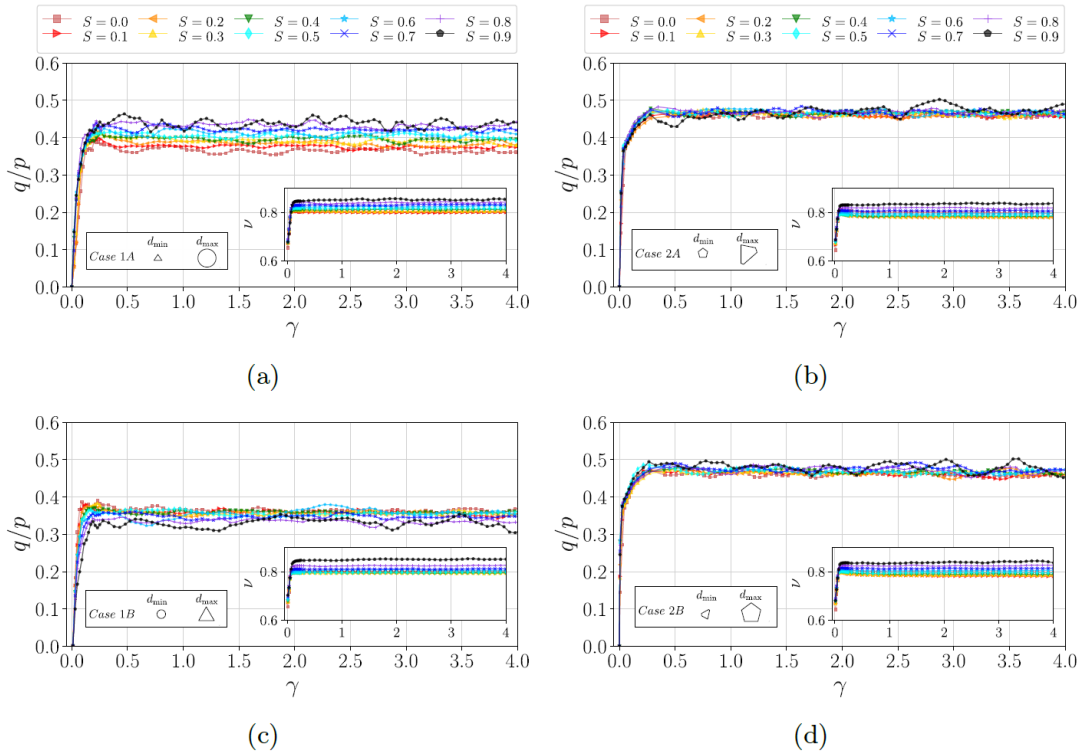

Figure 5: Evolution of solid fraction ν (inset) and the shear strength q/p for Case 1 (left) and Case 2 (right) as a function of the shear deformation γ.

In order to highlight these observations, we modified line 273 as follows:

L273: [...] For the shear stress q/p, we observe a gradual gain of resistance in all the cases up to γ õ.2. Then, a transient zone towards the steady state takes place that varies depending on the material. While in Case 1A the steady state is reach around γ õ.4, in case 1B the stabilization occurs more rapidly, as soon as γ õ.3. For the Cases 2A and 2B, the shear strength stabilization occurs practically at the same levels of deformation (i.e., γ õ.3). In terms of volume of the sample, we observe that in all cases the solid fraction finds steady values earlier than the shear strength, around γ õ.25.

5. The coordination number Z = 2Nc/Np is it the mechanical coordination number? Because as far as I remember, mechanical CN has a slightly different formulation that stated here.

A5. We thank the Referee for pointing out this difference. Slightly different definitions for the coordination number can be found in the literature, being that one of the mechanical coordination number by Thornton [2].

$$Z_m = \frac{2C - N_1}{N - N_1 - N_0}, \tag{5}$$

being C the number of contacts, N the number of particles, N_1 and N_0 are the number of particles with only one or no contacts, respectively. The coordination number employed in this work is defined as:

$$Z = \frac{2N_c}{N_p^*}, \tag{6}$$

where N_c is the total number of force-bearing contacts (i.e., all contact with non-zero force), and N_p^* is the number of grains transmitting forces (i.e., all particles having two or more active contacts). Consequently, there exists a subtle distinction between the two quantities related to the treatment of N_1 in Equation (5). In order to illustrate this, a comparison between the evolution of Z and Z_m for Case 1A and Case 1B is shown in Figure 6. It can be observed that Z_m is consistently higher

Z by a small margin. This difference arises due to the absence of gravity in our simulations. In scenarios where gravity is activated, both parameters should converge to the same values. Nevertheless, both Z_m and Z exhibit analogous trends with S, enabling us to draw similar conclusions regardless of the chosen parameter.

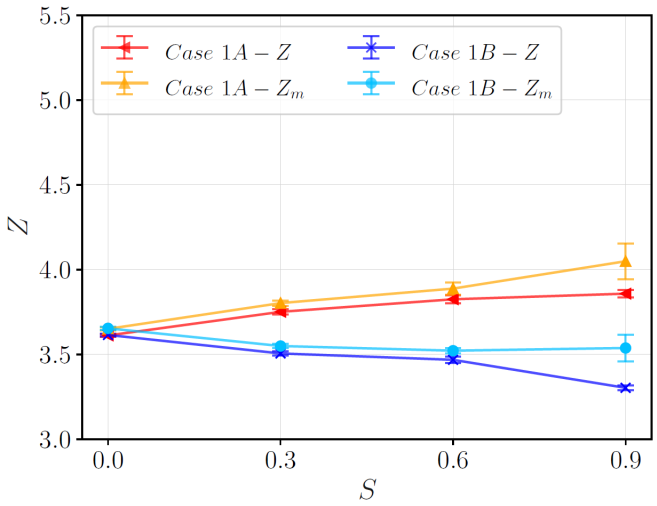

Figure 6: Evolution of Z and Z_m for Case 1A and 1B.

6. I would also like to see a couple of q/p profile against the axial strain for some cases as they impart a lot of information on strain hardening/softening tendency. Or the variation of the CN against axial strain.

A6. We modified Figures 9 and 10 in the manuscript to include the complete profile of q/p as a function of the shear deformation γ (Figure 5 below), where no softening is observed in any sample. Note that the shear deformation is defined as $\gamma = \delta_x/h$, being δ_x the cumulated horizontal displacement of walls in the direct shear test, and h the height of the sample. Figure 7 below shows the evolution of Z as a function of γ. We observe a gradual increase of the coordination number in all cases up to γ 0.2 - 0.3. In contrast to the macroscopic behavior, the microstructural descriptors such as Z require a higher level of deformation to reach steady state behavior.

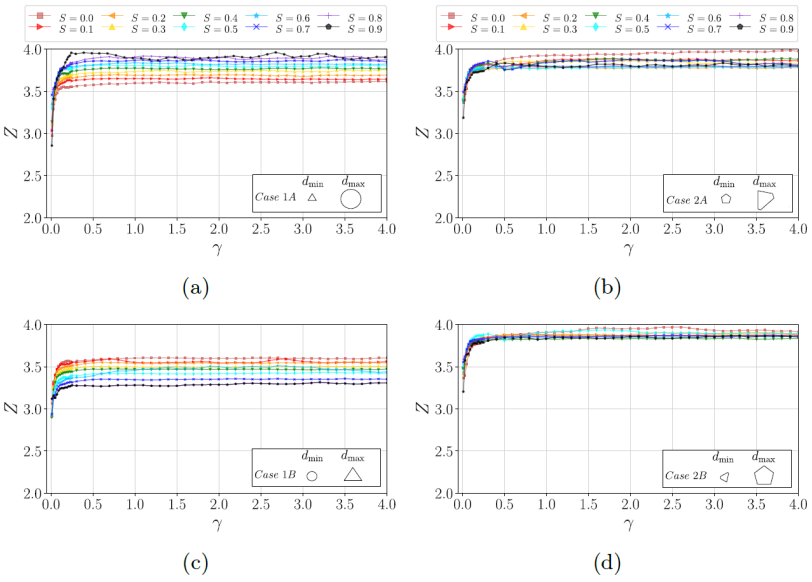

Figure 7: Evolution of coordination number Z for Case 1 (left) and Case 2 (right) as a function of the shear deformation γ.

Responses to the Reviewer C

We thank the Referee for the attentive reading of our manuscript and the useful comments. Please find each of the comments (#) followed below by our answers (A#).

1. It would be good to clarify what is exactly the system when S=0. For case A 1A for example, is it a mixture of the 10 shapes, all with the same 'diameter'? Then the total area of each shape would need to be the same, leading to more triangles than 64-sides polygons. Is that correct?

A1. In samples where $S = 0$, the circles that circumscribe each particle in the sample are the same size. The Referee is right at pointing out that, in a such case, the samples contain more triangles than any other shape given the uniform distribution of particle size by area.

For the sake of clarity, we added a new sentence in line 147 as follows:

L147: [...] (note that a polygonal grain size is defined by the diameter of the circle that circumscribes the polygon)

2. Tying up to the previous question, I find the drop in Fig. 9b between S=0 and S=0.1 quite surprising, and inconsistent with the rest of the trend. Any idea why the volume fraction is changing so much when adding a little polydispersity for the irregular pentagons, while it was pretty stable for the cases with different shapes?

A2. We thank Referee for this remark. It is certainly surprising that adding a little polydispersityseems to have a larger impact in Cases 2A and 2B, while such behavior is not observed in Cases 1A and 1B.

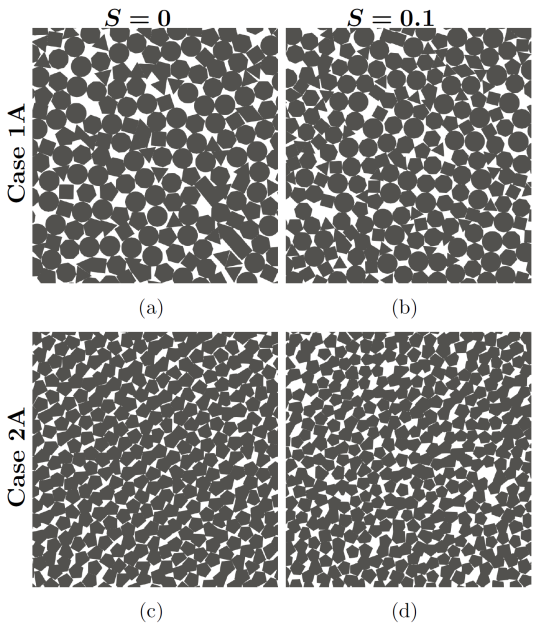

Figure 8: Screenshot of samples with particle size span $S = 0$ (left) and $S = 0.1$ (right) for Case 1A and Case 2A.

For 2D assemblies composed of disks, when the particles are strictly monodisperse, they can self-organize into a highly compact arrangements. However, a slight deviation in particle sizes disrupts this crystalline arrangement in favor of random configurations [18, 19, 13]. This phenomenon is observed in grain assemblies where particle shape is quite similar, which helps to explain why the drop in the solid fraction is not observed in the case with different shapes (Case 1A and 1B). Nevertheless, we can still observe an initial decrease of v for Case 2, where particle shape is relatively similar. Figure 8 shows a screenshot of the concerned samples, confirming that Case 2A develops a relatively ordered packing that explains the drop pointed out by the Referee. Despite this behavior in terms of solid fraction, no major variations are observed in shear strength in the critical state or other parameters, allowing us to compare the whole range of grain size spans tested

without concerns about the possibility of proving the properties of a crystalline packing.

3. It is a missed oportunity in my mind not to show the beginning of the simulations before reaching critical state in figure 7. It is nice to see that the steady state is reached and stable, but there would be room to show how we got there.

A3. We thank the Referee for this comment. In effect, we added the curves for shear strength q/p and solid fraction ν as a function of the shear deformation from the beginning of the simulations (Figs. 7 and 8 in the manuscript; the figures are also added in Fig. 5 below).

For the shear strength q/p, we observe a gradual gain of resistance in all the cases up to γ ̃0.2. Then, a transient zone towards the steady state takes place that varies depending on the material. While in Case 1A the steady state is reach around γ ̃0.4, in case 1B the stabilization occurs more rapidly and as soon as γ ̃0.3. For Cases 2A and 2B, the shear strength stabilization occurs practically at the same levels of deformation (i.e., γ ̃0.3). In terms of volume of the sample, the solid fraction finds steady values generally earlier than the shear strength.

In order to highlight these observations, we modified line 273 as follows:

L273: [...] For the shear stress q/p, we observe a gradual gain of resistance in all the cases up to γ ̃0.2. Then, a transient zone towards the steady state takes place that varies depending on the material. While in Case 1A the steady state is reach around γ ̃0.4, in case 1B the stabilization occurs more rapidly, as soon as γ ̃0.3. For the Cases 2A and 2B, the shear strength stabilization occurs practically at the same levels of deformation (i.e., γ ̃0.3). In terms of volume of the sample, we observe that in all cases the solid fraction finds steady values earlier than the shear strength, around γ ̃0.25.

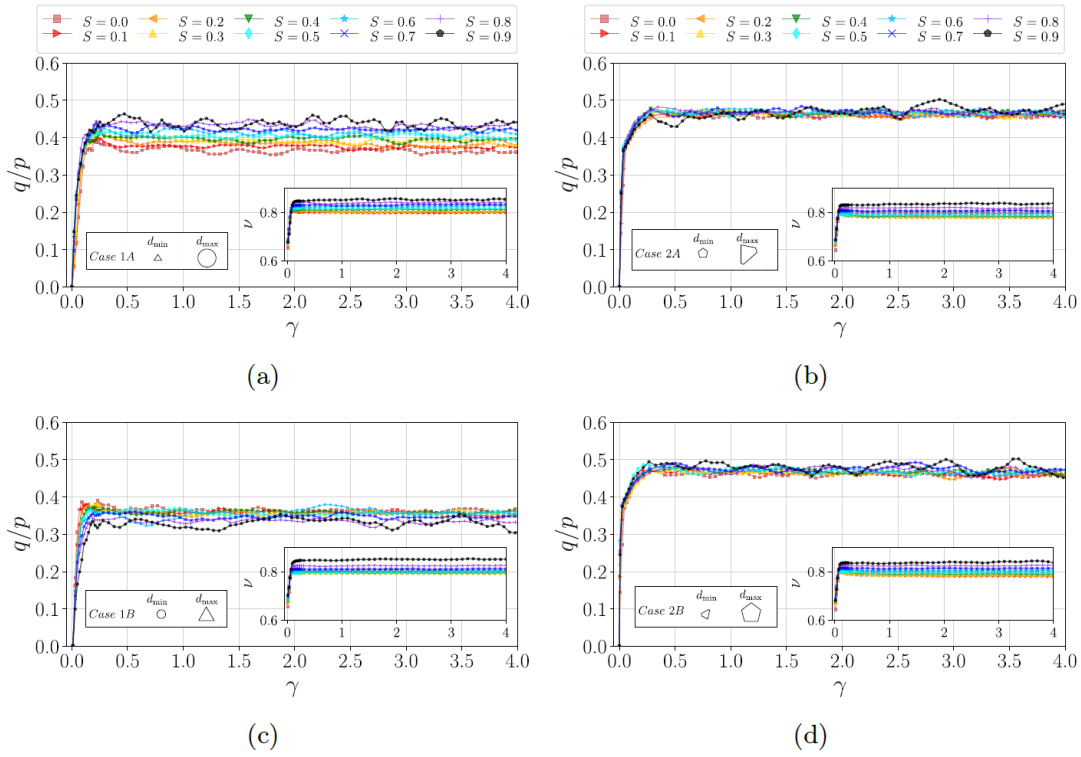

Figure 9: Evolution of shear strength q/p and solid fraction ν (inset) for Case 1 (left) and Case 2 (right) as a function of the shear deformation γ.

4. Part of the discussion on how Zf depends on the size and sharpness should consider that for the same dr, the length of the side of the particle depends on the number of sides of the polygon. Triangles have intrinsically less surface to establish contact than disks for a given circumscribing diameter. Therefore it may be good to also show the distributions of Zf as

a function of perimeter length, to distinguish between the size effect and the sharpness effect on Zf. Also, the case S=0 is absent from the graphs in Fig 11, but there could still be differences in Zf between the different shapes of equal diameter grains (if my interpretation in (1) is correct), and it would be good to report it too.

A4. We thank the Referee for these remarks. We added the case $S = 0$ in Figures 11 and 12 of the manuscript to show the differences in Z_f between the different shapes of equal particle diameters.

In addition, Figure 10 below shows the evolution of Z_f as a function of the particle perimeter (C) as suggested by the Referee. While it is true that triangles have intrinsically less 'surface' to establish contact than equivalent-size disks (as shown in Figures 10 (a) and (c)), we observe that the dispersion of particle sizes has a more significant effect on Z_f than particle shape, being the larger particles always better connected than smaller ones. If we compare Z_f of Cases 1A and 1B, larger particles with high n_s are slightly better connected than larger sharper particles.

In turn, if we focus on small particles, we observe that sharper grains are better connected than those with larger n_s. This unexpected result is related to the fact that small sharp corners can reach neighboring particles that are unreachable for less angular grains [4]. To include the role of particle's perimeter in the analysis of connectivity, we added inset plots in the figures of Z_f based on Wadell's circularity [3], which relates the perimeter of the particle to that of the corresponding circumscribing circle. In these figures for Case 1A and 1B, we can observe that larger particles with high ns are always better connected than larger sharper particles, as opposed to the smaller particles where less circular grains tend to be more connected.

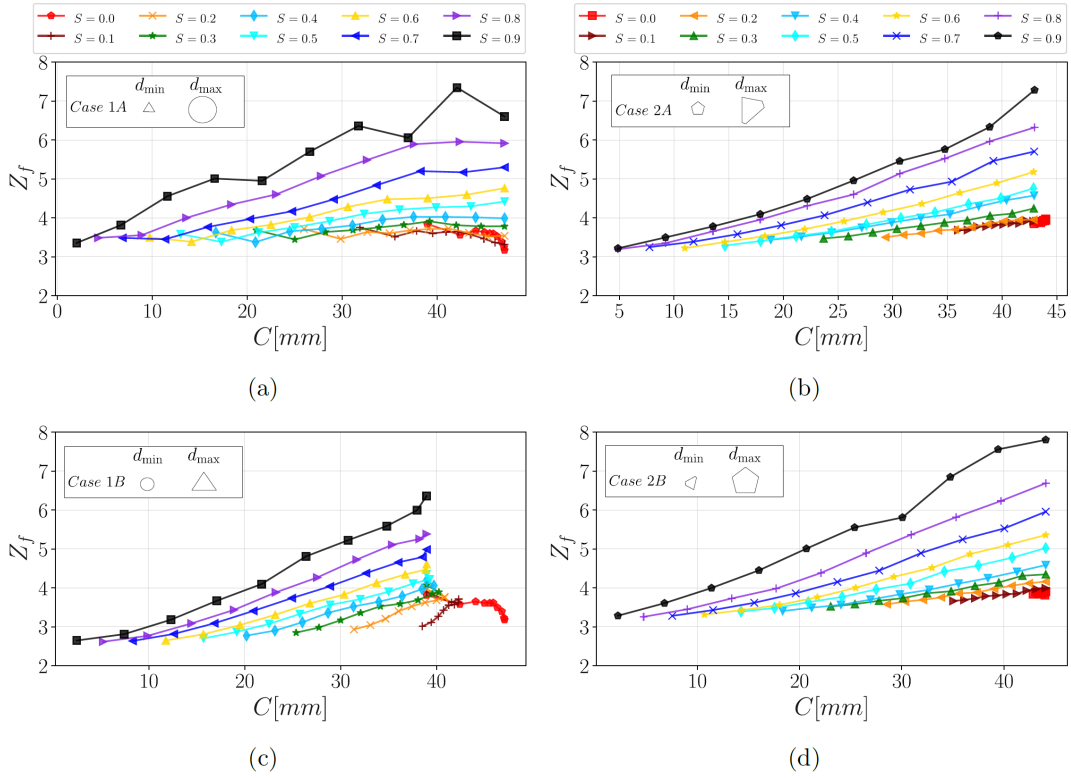

Figure 10: Evolution of Z at critical state as a function of the particle perimeter (C) and for Case 1A (a), Case 1B (c), Case 2A (b) and Case 2B (d).

5. Considering the vertex-side and side-side split of the stresses (Fig. 15), these reproduce the behaviour of the number of contacts. Is there any difference in the typical intensity of the forces that each type of contact carries?

A5. To adress this question, we computed the average force per type of contact as follows:

$$<F_N^{sv}> = \frac{\sum_{i=1}^{N_{sv}} F_N}{N_{sv}}, <F_N^{ss}> = \frac{\sum_{i=1}^{N_{ss}} F_N}{N_{ss}}, <F_N^{c}> = \frac{\sum_{i=1}^{N_{c}} F_N}{N_{c}}, \quad (7)$$

being $<F_N^{sv}>$ and $<F_N^{ss}>$ the average normal force for side-vertex and side-side contacts, respectively. $<F_N>$ is the average normal force considering all the contacts.

Figure 11 shows the evolution of $<F_N^{ss}>$ and $<F_N^{sv}>$, normalized by the average normal force as a function of the grain size dispersion S, for Cases 1A and 1B (a), and Cases 2A and 2B (b). In Case 2A and Case 2B, both contact types carry similar normal forces, which remain close to the global average. On the other hand, in Case 1A and 1B, while $<F_N^{ss}>/<F_N>$ remains fairly constant for all samples, the side-vertex contacts (c^{ss}) show a gradual increase in the average intensity of forces as S grows.

The behavior of these force averages is indeed quite different from the behavior of the stresses carried by each contact family (Figure 15 in the manuscript). We understand these differences due to the multiple factors involved in the computation of stresses, including the distance between the center of the particles in interaction, the contact points locations, and the contact distribution on the particle surface. As the stress partition by contact type is more relevant for strength analysis, we have decided not to extend the discussion on average contact forces in the manuscript.

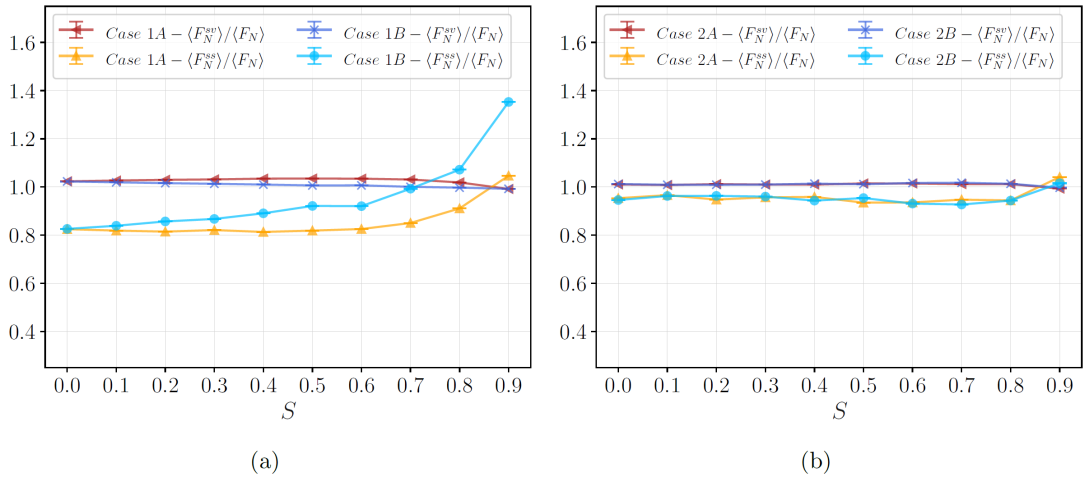

Figure 11: Evolution of the average of normal forces per contact type ($<F_N^{ss}>$ and $<F_N^{sv}>$) normalized by average normal force per contact at critical state as a function of the grain size dispersion S for Cases 1A and 1B (a), and Cases 2A and 2B (b).

6. I need clarification on how the stress partition by shape is performed. How are the q^i computed? Does this include any contact with one of the particles of the given shape? Also, it would be interesting to report the normal stress partition as well as the deviatoric stress, since a priori there is no reason to have equipartition of the stresses between species. Actually, regarding normal stress and pressure, would it be possible to also show (maybe in figure 7) how well the prescribed pressure is maintained and how close p and P are to each other?

A6. In order to add clarity to this part of the manuscript, we added the next sentence in line 497:

L497: being q^i the deviatoric component of the granular stress tensor σ_i for each particle *shape class (sc)* in the assembly. This tensor is computed using the following expression:

$$\sigma^i_{mn} = \frac{1}{A} \sum_{\forall N_p^{*i}} f_m^c r_n^c, \tag{8}$$

where N_p^{*i} is any load-bearing grain with a given shape 'i', f_m^c is the m component of the force at contact c, and r_n^c is the n component of the vector joining the center of mass of particle and the contact point. We use the principal stresses of σ^i (i.e., σ_1^i and σ_2^i) to calculate $q^i = (\sigma_1^i - \sigma_2^i)/2$ and $p^i = (\sigma_1^i + \sigma_2^i)/2$ for each family shape.

Stress partition q^i/q: using equation (8) we compute q^i and p^i by shape class to analyze the stress partitions, as suggested by the Referee. Figure 12 below shows the evolution of the ratio between deviatoric stress by shape class q^i and the total

deviatoric stress q for Case 1 and Case 2. For $S = 0$, we observe that each shape class supported a similar level of total desviatoric stress q^i/q õ.1, with the exception of triangular particles. Nevertheless, as the value of S increases, it is observed that smaller particles decrease their contribution while larger particles increase their contribution influenced by their shape. The trend shown by q^i/q is almost similar to the one shown by q^i/p.

Stress partition p^i/p: Figure 13 shows the evolution of the ratio between mean stress by shape class and the total mean stress p^i/p for all samples. For mono-disperse samples ($S = 0$), each shape class supported a similar level of total normal stress p^i/p õ.1. Therefore, each family supported a similar amount of the total mean stress. However, as the value of S increases, it is observed that smaller particles decrease their contribution while larger particles increase their contribution as compensation mechanism.

Pressure in the assemblies: Figure 14 below shows the evolution of the ratio between p and prescribed pressure P. As observed, the mean values of p/P for all simulations is close to 1. This mean that the applied vertical stress is well maintained in the sample.

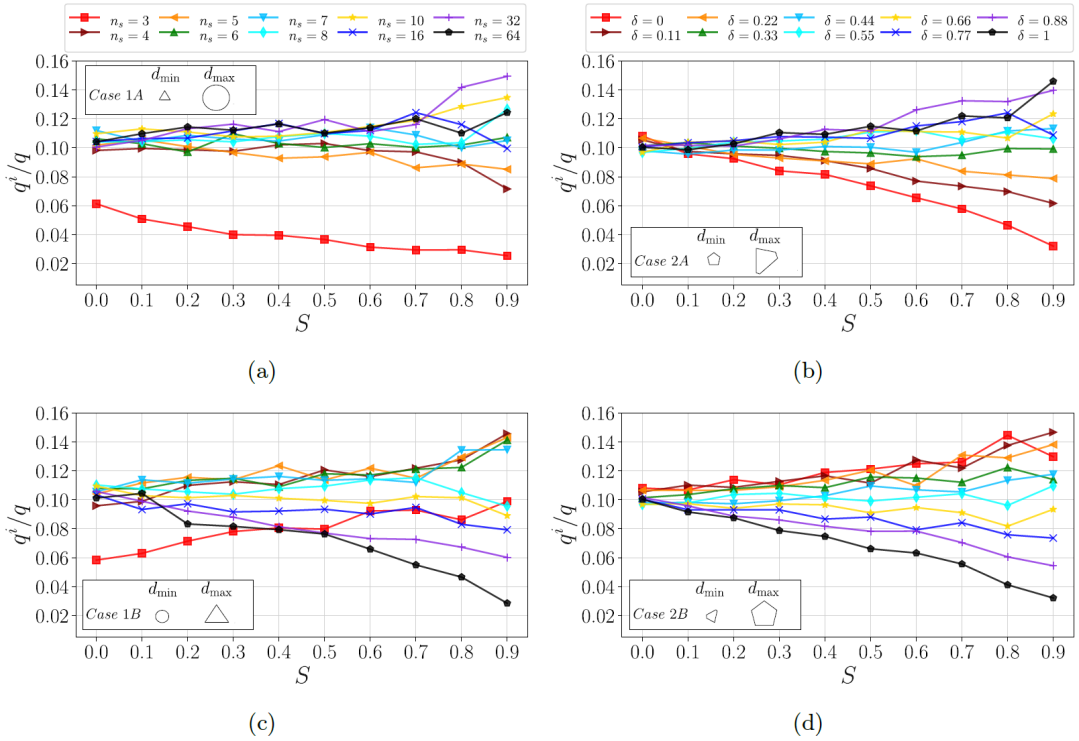

Figure 12: Decomposition of the deviatoric component of stresses by shape class for Cases 1 (left) and Case 2 (right) as a function of the grain size span S.

7. The mathematical definition of the 'regularity' of the pentagons given in eq. (1) is not specified enough. Is the plus-minus sign based on the value of k? For delta=1, which is used in some simulations, the equation would generate a triangle, which is not what Fig. 2 shows.

A7. We thank the referee for this remark that made us aware of an error in equation (1) in the manuscript. The correct form of the equation is

$$\theta_k = \theta_0 + k\frac{2\pi}{5} \pm \frac{\pi}{5} r_{[0,\delta]}, \tag{9}$$

a random variable in the range $[0,\delta]$, δ is the degree of irregularity that can vary from 0 to 1, and the $\pm$ sign is also randomly chosen for each vertex [20]. This equation has been corrected in the manuscript in line 132 and its description is corrected in line 133 as follows

L133 [...] being $r_{[0,\delta]}$ a random variable in the range $[0,\delta]$, δ is the degree of irregularity that can vary from 0 to 1, and the $\pm$ sign is randomly chosen for each vertex.

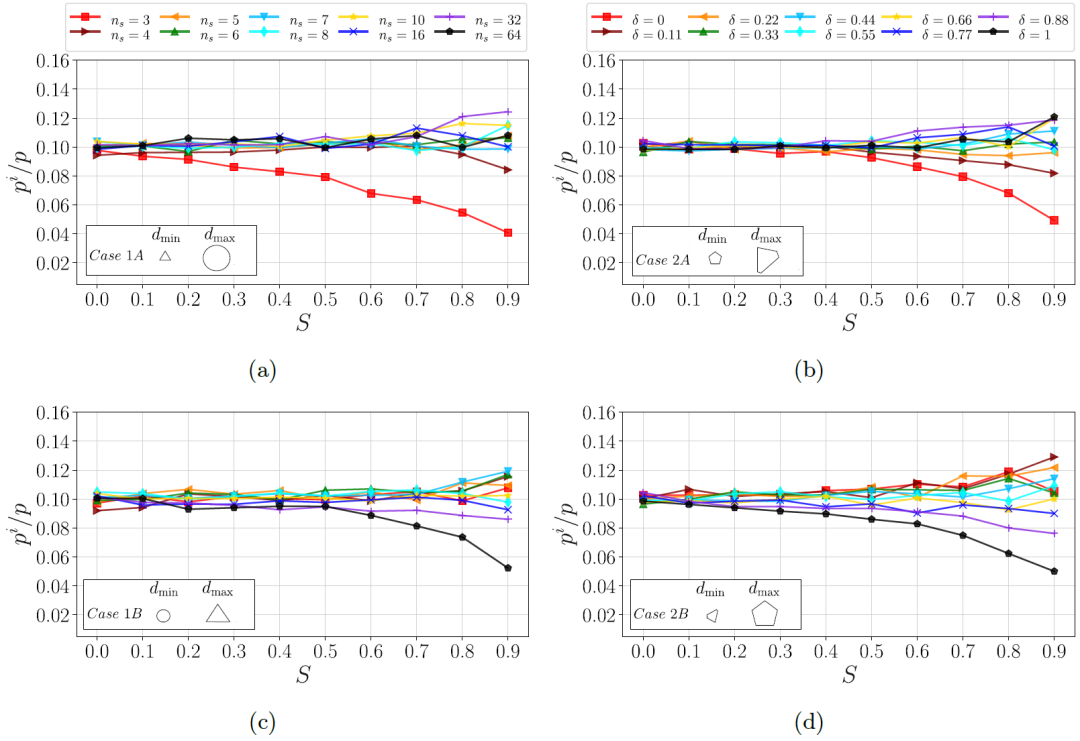

Figure 13: Decomposition of the mean component of stresses by shape class for Cases 1 (left) and Case 2 (right) as a function of the grain size span S.

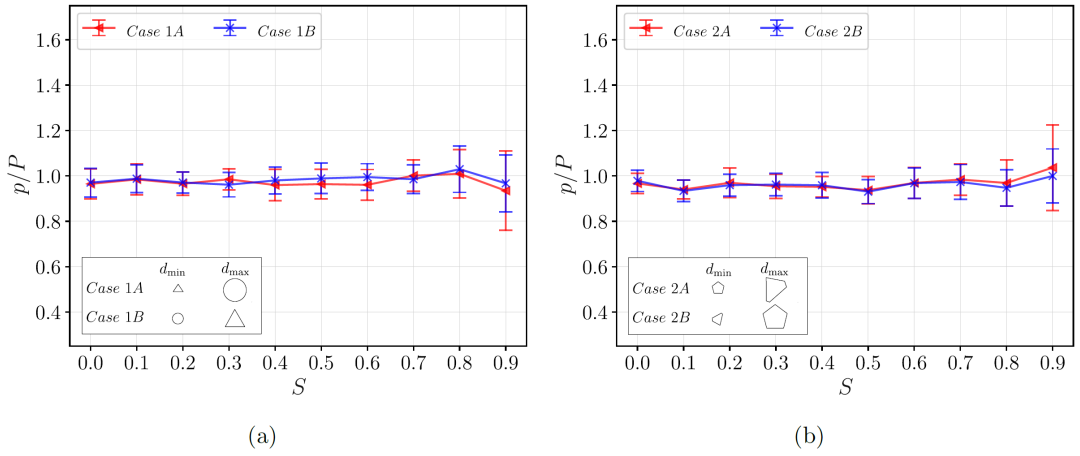

Figure 14: Evolution of the ration of p/P for Cases 1 (a) and Cases 2 (b).

8. Eq. 3 and Eq. 6 basically define two different notation for the same quantity. It would be clearer to introduce first the relative diameter dr, and then rewrite equations 3 and 4 in terms of this dr as either $\delta = dr$ or $\delta = 1 - dr$.

A8. We thank the referee for this recommendation. In effect, we moved the definition of parameter dr to the line 170, and modified the corresponding equations for Case 2A and Case 2B that describe the level of irregularity of the particle shapes as follows

- For Case 2, the following equations characterize the level of irregularity as a function of the relative grain diameter in the assembly dr, defined as:

$$dr = \frac{d - d_{min}}{d_{max} - d_{min}}. \tag{10}$$

Note that this reduced diameter varies between 0 and 1, as the grain belongs to either the smaller or larger classes of particles in the assembly. When the large grains are the most irregular ones the irregularity is equal to $\delta(d) = dr$ (Case 2A), and when the large grains are the most regular ones, $\delta(d) = 1 - dr$ (Case 2B).

Miscellaneous

We thank the referee for the miscellaneous comments. The corresponding modifications were made in the manuscript.

- Fig. 3 caption: The writing is a bit unclear, suggesting that S is normalised by d_{max} (while it is d that is normalised).
- L192: "As/A" -> "A_s/A"
- L204: which kind of average is considered here for $<d>$, the area average?
  A. The average $<d>$ is computed using the diameters of the circumscribed circles of each particle. This calculation includes all particles regardless of whether they are carrying force or not.
- Fig 6 caption: "x' axis" -> "x axis"
- L217: "as they were glued" -> "as if they were glued"
- Fig. 11a inset y-label: "C_0" -> "c_0"
- L550: "q_{sc}" -> "q^i"

References

[1] S. Carrasco, D. Cantor, and C. Ovalle. Effects of particle size-shape correlations on steady shear strength of granular materials: The case of particle elongation. *Int. J. Numer. Anal. Methods. Geomech.*, 46(5):979–1000, 2022.

[2] C. Thornton. Numerical simulations of deviatoric shear deformation of granular media. *Géotechnique*, 50(1):43–53, 2000.

[3] H. Wadell. Sphericity and roundness of rock particles. *J. Geol*, 41(3):310–331, 1933.

[4] E. Azéma, N. Estrada, and F. Radjai. Nonlinear effects of particle shape angularity in sheared granular media. *Phys. Rev. E*, 86(4):041301, 2012.

[5] T. L. Youd, D.R. Nichols, E.J. Helley, and K.R. LaJoie. Liquefaction potential of unconsolidated sediments in the southern san francisco bay region, california. Technical report, US Geological Survey, 1973.

[6] J. Zheng and R.D. Hryciw. Index void ratios of sands from their intrinsic properties. *J. Geotech. Geoenviron.*, 142(12):06016019, 2016.

[7] S. Amirpour H., M. Karray, M. N. Hussien, and M. Chekired. Influence of particle size and gradation on shear strength–dilation relation of granular materials. *Can. Geotech. J.*, 56(2):208–227, 2019.

[8] A. Deiminiat, L. Li, F. Zeng, T. Pabst, P. Chiasson, and R. Chapuis. Determination of the shear strength of rockfill from small-scale laboratory shear tests: A critical review. Adv. Civ. Eng., 2020, 2020.

[9] A. B. Cerato and A. J. Lutenegger. Specimen size and scale effects of direct shear box tests of sands. *Geotech. Test. J.*, 29(6):507–516, 2006.

[10] B. O. Hardin. Crushing of soil particles. *J. Geotech. Eng.*, 111(10):1177–1192, 1985.

[11] P. V. Lade, J. A. Yamamuro, and P. A. Bopp. Significance of particle crushing in granular materials. *J. Geotech. Eng.*, 122(4):309–316, 1996.

[12] C. Ovalle, C. Dano, P.-Y. Hicher, and M. Cisternas. Experimental framework for evaluating the mechanical behavior of dry and wet crushable granular materials based on the particle breakage ratio. *Can. Geotech. J.*, 52(5):587–598, 2015.

[13] C. Voivret, F. Radjai, J-Y Delenne, and M. S. El Youssoufi. Space-filling properties of polydisperse granular media. *Phys. Rev. E*, 76(2):021301, 2007.

[14] R. Jullien, A. Pavlovitch, and P. Meakin. Random packings of spheres built with sequential models. *J. Phys. A Math. Theor.*, 25(15):4103, 1992.

[15] W. M. Visscher and M. Bolsterli. Random packing of equal and unequal spheres in two and three dimensions. *Nature*, 239:504–507, 1972.

[16] A. N. Schofield and P. Wroth. *Critical state soil mechanics*, volume 310. McGraw-hill London, 1968.

[17] K. H. Roscoe. The influence of strains in soil mechanics. *Géotechnique*, 20(2):129–170, 1970.

[18] J.G. Berryman. Random close packing of hard spheres and disks. *Phys. Rev. A*, 27(2): 1053, 1983.

[19] S. Torquato, T. M. Truskett, and P. G. Debenedetti. Is random close packing of spheres well defined? *Phys. Rev. Lett.*, 84(10):2064, 2000.

[20] D.-H. Nguyen, E. Azéma, P. Sornay, and F. Radjai. Effects of shape and size polydispersity on strength properties of granular materials. *Phys. Rev. E*, 91(3):032203, 2015.

Review Round 2

Reviewer 1 (Vasileios Angelidakis)

I appreciate the new graphs provided by the authors in response to my review. Using shape parameters that we can apply in the real world is important if we want shape characterisation to become a comprehensive tool to understand real granular systems. I found surprising that these graphs did not appear in the revised manuscript, but that is not a problem overall. I am supportive of this work being published in its current form.

Reviewer 2 (Debdeep Sarkar)

No further comments from my side. Can be accepted for publication.

Reviewer 3 (Francois Guillard)

In the revised version of their manuscript, the authors carefully considered all the comments from the reviewers and provided high quality answers and new analysis to address in detail thoses comments. I think the few points of clarification that were needed in the manuscript have been properly addressed; I have no further comment and I support publication in Open Geomechanics.

Author Response

Great, please publish it.